Publications of the Astronomical Society of the Pacific, 129:124203 (7pp), 2017 December https://doi.org/10.1088/1538-3873/aa9004

A Refined Radial Velocity Curve for the L Dwarf Donor of WZ Sagittae*

Thomas E. Harrison
Department of Astronomy, New Mexico State University, Box 30001, MSC 4500, Las Cruces, NM 88003-8001, USA; tharriso@nmsu.edu
Received 2017 August 25; accepted 2017 September 29; published 2017 October 25

Abstract

We have obtained a radial velocity curve for the L dwarf donor in WZ Sagittae using phase-resolved *J*-band spectra obtained with GNIRS on Gemini-north. We find a radial velocity semi-amplitude of $K_2 = 525 \pm 11$ km s^{-1}. This result reduces the error bar by a factor of three over previous attempts. A relatively strong, unidentified emission line centered near 1.177 μm, corrupts the blue K I doublet in these data. While an H I emission feature near 1.2527 μm distorts the depth of the red K I doublet. In addition, a weak H I emission line at 1.1969 μm falls in the middle of the strongest FeH feature in these spectra. The combination of these contaminants prevents us from precisely constraining the spectral type of the donor. The strength of the absorption features remains consistent with an early L spectral type.

Key words: stars: dwarf novae

Online material: color figures

1. Introduction

WZ Sge is an ultra-short period cataclysmic variable (CV) that has rare, long lasting, large amplitude outbursts (Patterson et al. 2002). It is also one of the closest of all CVs, with an astrometric distance of 43 pc (Thorstensen 2003; Harrison et al. 2004). Even though it is nearby, and has a very low accretion rate (Patterson 1998), unraveling the precise nature of the binary components in WZ Sge has been difficult. It is important to characterize the spectral type and mass of the donor to place the system in an evolutionary context. The standard paradigm for CV evolution states that after a common envelope phase that leads to the formation of a semi-detached binary, the accretion of material onto the white dwarf primary from the companion over time results in a continuous decrease in the mass of the donor. Angular momentum loss processes (e.g., King & Kolb 1995) keep the system in contact, and drives the system to shorter, and shorter periods. Eventually, the donor star becomes degenerate, and further mass transfer leads to an increase in the orbital period of the system. This is the so-called "period bounce," and occurs near an orbital period of ~70 minutes (c.f., Kolb & Baraffe 1999). The expectation is that the donors in post-period bounce systems should have very low masses ($M_2 \leqslant 0.05\,M_\odot$), and very late spectral types near the L/T dwarf boundary (Knigge et al. 2011).

Steeghs et al. (2001) provided the first constraints on the nature of the secondary by constructing a radial velocity curve for the donor using narrow Hα emission lines induced by irradiation of the companion from the luminous accretion disk during its 2001 outburst. They were able to limit the radial velocity semi-amplitude of the secondary star to the range $493\,\mathrm{km\,s^{-1}} \leqslant K_2 \leqslant 585\,\mathrm{km\,s^{-1}}$. With these limits, and an estimate of the primary star's radial velocity semi-amplitude of $K_1 = 37 \pm 5\,\mathrm{km\,s^{-1}}$, they found that the mass of the donor star in WZ Sge was close to the stellar/sub-stellar boundary. Harrison et al. (2013) modeled infrared light curves of WZ Sge and found a best fitting donor star temperature of $T_{\rm eff} = 2000$ K, consistent with a spectral type near L2. Harrison (2016a) then used phase-resolved *K*-band spectroscopy to derive a radial velocity curve using the CO absorption features of the donor. With the radial velocity semi-amplitude of $K_2 = 520 \pm 35\,\mathrm{km\,s^{-1}}$ fixed, phasing of the data revealed a spectrum for the companion that was consistent with an early L dwarf spectral type.

The radial velocity curve of the donor found by Harrison (2016a) was complicated by CO emission from the accretion disk. Except for the CO features, the *K*-band spectra of L dwarfs show no strong lines that could aid in spectral classification, nor allow for a more precise radial velocity curve to be measured. For L dwarfs, the *J*-band provides strong atomic absorption lines from potassium, and this bandpass does not contain significant CO emission. We have used GNIRS[1] on Gemini-north to obtain phase-resolved *J*-band spectroscopy of WZ Sge. From these data we derive a more precise radial

* Based on observations obtained at the Gemini Observatory, which is operated by the Association of Universities for Research in Astronomy, Inc., under a cooperative agreement with the NSF on behalf of the Gemini partnership: the National Science Foundation (United States), the National Research Council (Canada), CONICYT (Chile), Ministerio de Ciencia, Tecnología e Innovación Productiva (Argentina), and Ministério da Ciência, Tecnologia e Inovação (Brazil).

[1] http://www.gemini.edu/sciops/instruments/gnirs/

velocity semi-amplitude for the donor. With this result, and previously published measurements of the semi-amplitude for the white dwarf primary, we are able to show that the properties of the donor in WZ Sge remains consistent with an early-type L dwarf. In the next section we discuss the data set, in Section 3 we present our results on the radial velocity curve and spectral type of the donor, and in Section 4 we discuss these results and derive our conclusions.

2. Data

WZ Sge was observed using GNIRS on Gemini north on 2016 July 11 and 2016 July 12. On the 11th it was observed from 08:28 until 10:27 UT, and on the 12th, data was obtained from 08:37 to 9:27 UT. The G110 grating and short blue camera were used in single order, long slit mode, with the grating set to cover the wavelength interval of $1.16 \leqslant \lambda \leqslant 1.27\,\mu$m. The dispersion was 1.11 Å/pix, however, a wider slit ($0\farcs675$) than the default ($0\farcs3$) was used to increase throughput at the expense of the full resolution that the G110 grating is capable of delivering. The data here have $\Delta v \simeq 94\,\mathrm{km\,s^{-1}}$. The seeing on both nights was about $0\farcs5$.

The exposure times for WZ Sge were kept short, 180 s ($\Delta\phi = 0.037$), to limit orbital smearing. Depending on how many spectra were medianed together in each phase bin, the signal-to-noise ratio (S/N) in the continuum at 1.2 μm for the binned spectra ranged between 50 and 60. To allow for accurate wavelength calibration, arc lamps were obtained every dozen exposures, or so. The A0V star HD 182761 was observed each night for telluric correction. The chosen spectral range is free from significant telluric absorption, so a single telluric standard each night proved sufficient. The data were reduced in the standard fashion using IRAF. The images were first bias-subtracted and flatfielded using the calibration data for our program. The standard ABBA observing scheme was used. Difference images were then constructed by subtracting the B-beam image from the A-beam, and vice versa. The spectra were extracted from these difference images using the IRAF task *apall*, and these were wavelength calibrated using the arc lamp exposures. Each segment of data fell between two arc lamp exposures, and we used the wavelength solutions for both arcs (within the IRAF task *dispcor*) to attempt to obtain the most accurate wavelength calibration possible.

An exquisitely precise orbital ephemeris for WZ Sge exists (Patterson et al. 1998). This is due to the presence of partial eclipses in its light curve. These eclipses, however, are not of the primary star, but of the accretion hot spot. Thus, the time of inferior conjunction occurs before the eclipse. Skidmore et al. (2002) proposed that the true time of binary phase 0 is $\phi = 0.954$ when using the Patterson et al. ephemeris. We have used this offset when phasing our data.

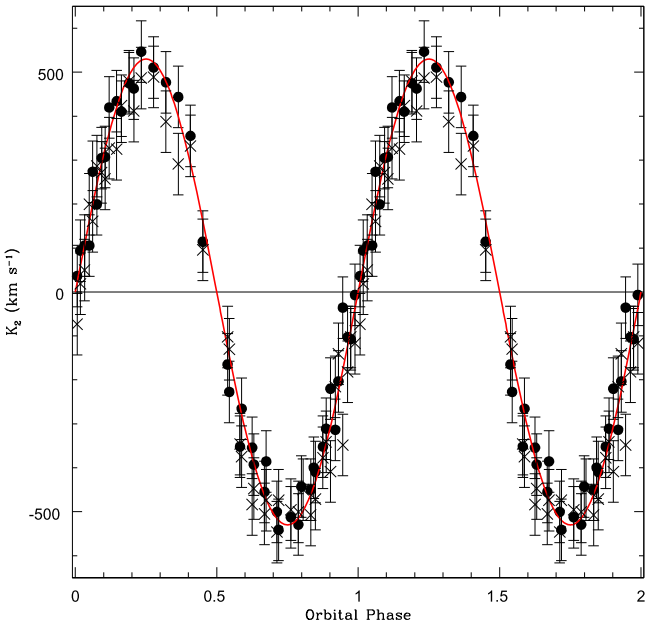

Figure 1. Radial velocity curve of the donor of WZ Sge. The crosses are the data for the K I line at 1.2432 μm, and the filled circles are for the K I line at 1.2522 μm. The χ^2 analysis (see Figure 2) finds a best fitting velocity of $K_2 = 525 \pm 11\,\mathrm{km\,s^{-1}}$ (red curve). A systemic velocity of $\gamma = -72\,\mathrm{km\,s^{-1}}$ (see Steeghs et al. 2001) centers the data set. The error bars on the individual data points are $\pm 70\,\mathrm{km\,s^{-1}}$.
(A color version of this figure is available in the online journal.)

3. Results

3.1. The Radial Velocity of the Donor

To derive a radial velocity curve for the donor in WZ Sge we used the red K I doublet ($\lambda\lambda$1.2499, 1.2550 μm). We measured the positions of both of these lines using the *splot* task in IRAF. The radial velocity curve is shown in Figure 1. We plot the measurements separately for each line. As noted above, we have offset the phasing of these data by $\Delta\phi = 0.046$. χ^2 analysis, Figure 2, finds a velocity semi-amplitude of $K_2 = 525 \pm 11\,\mathrm{km\,s^{-1}}$. Requiring $\chi^2_\nu = 1$ at the minimum, indicates that the error on our individual velocity measurements is $\sigma = 70\,\mathrm{km\,s^{-1}}$. Steeghs et al. (2001) found a systemic velocity of $\gamma = -72\,\mathrm{km\,s^{-1}}$. We have assumed that offset here.

Harrison (2016a) notes that it is likely that the donor in WZ Sge suffers from some level of irradiation. As described in Davey & Connon Smith (1992), the effect of irradiation of the secondary stars in CVs by the white dwarfs or accretion hot spots can skew the derived velocity amplitudes to higher values than reality. They suggest that limiting the data under analysis to the phase range $\phi = 0.8$ to $\phi = 0.2$, should lead to a more robust value for K_2. We have performed a χ^2 analysis on this

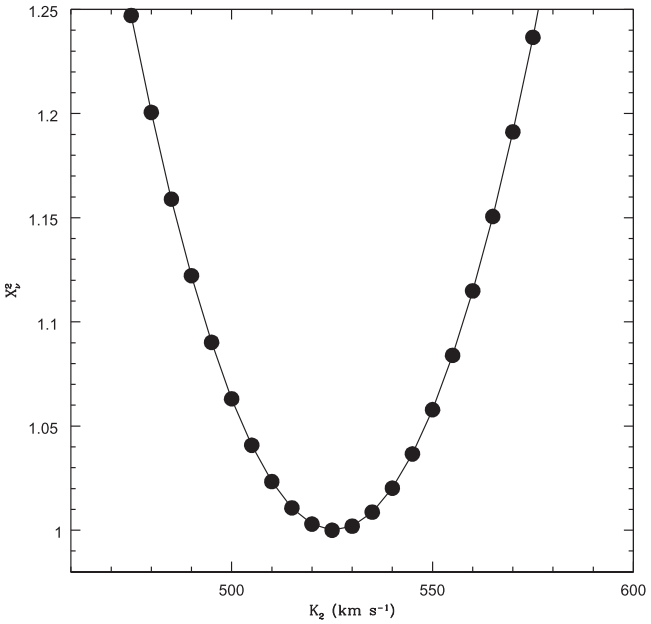

Figure 2. χ^2_ν values for a range in potential radial velocities for the donor star.

subset of the data and find an identical value for the radial velocity semi-amplitude to that derived above. This is almost certainly due to the fact that a large fraction of the data set fell within the proscribed phase interval.

With a relatively precise measurement of the radial velocity of the donor star, we Doppler corrected all of the spectra to the rest velocity of the secondary. In Figure 3, we plot those data in bins of $\Delta\phi = 0.1$ (except for $\phi = 0.4$, where only a single spectrum was obtained). For comparison, the spectrum of Kelu 1, an L2 dwarf, is also plotted in this figure (from McLean et al. 2007). The red K I doublet is easily visible at all phases in these data, though a broad emission feature redward of 1.24 μm skews the depth of the redder of these two absorption lines. Unfortunately, a relatively strong double-peaked emission line at $\lambda = 1.1758\,\mu$m, acts to obscure the bluer K I doublet at nearly all orbital phases. As shown in Figure 4, the morphology of this line behaves in a similar fashion to the He I and H I Brγ lines seen in *K*-band spectra of WZ Sge. At $\phi = 0.25$, this emission feature is blueshifted with respect to the secondary, and at $\phi = 0.75$ it is redshifted with respect to the secondary. We have seen this emission line in numerous other CVs, but it remains unidentified. From the NIST database,[2] potential sources for this feature are C I, N I, and Fe II. Howell et al. (2003) identified emission lines from C I in outburst *J*-band spectra of WZ Sge that are consistent with the position of this feature in the GNIRS data set.

[2] http://physics.nist.gov/PhysRefData/ASD

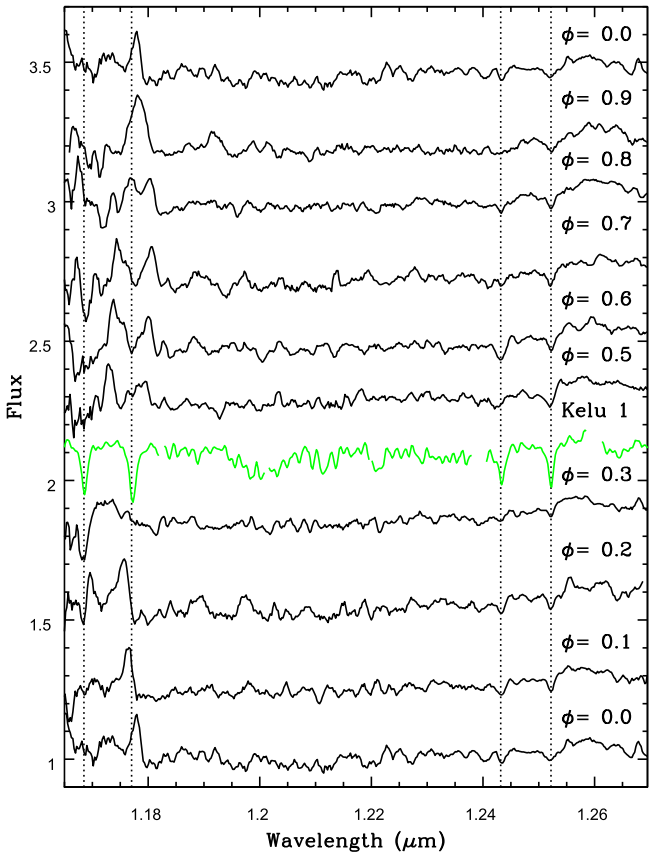

Figure 3. Doppler- corrected and phase-binned spectra of WZ Sge. From the bottom, the spectra run from $\phi = 0$, to $\phi = 0$, in steps of $\Delta\phi = 0.1$. Only a single spectrum was obtained at $\phi = 0.4$. Instead, we plot the spectrum of the L2 dwarf Kelu 1 (green) from McLean et al. (2007). The vertical dotted lines delineate the location of the two K I doublets. All of the WZ Sge spectra in this figure, and those that follow, have been boxcar smoothed by five pixels. (A color version of this figure is available in the online journal.)

3.2. The Spectral Type of the Brown Dwarf Donor

With the complete lack of an Na I doublet at 2.2 μm, significant CO absorption features, and other weak continuum features, Harrison (2016a) showed that the donor star in WZ Sge had to have a spectral type of L2 or later. With the presence of CO emission, and the lack of other strong absorption features in the *K*-band, tighter limits on the spectral type could not be extracted. The strong K I doublets, and the presence of broad FeH absorption, make the *J*-band the preferred spectral region for classifying L dwarfs. As shown in Mclean et al. (2003, their Figure 8), both the K I and FeH features weaken as one moves to later spectral types. The FeH features are very weak by L6. Mclean et al. found that the K I lines strengthen to a maximum near L4, and decline from there to a minimum at the L/T dwarf boundary. McGovern et al. (2004) found that the strength of the K I and FeH features are also gravity dependent, with both being substantially weaker for a lower gravity object.

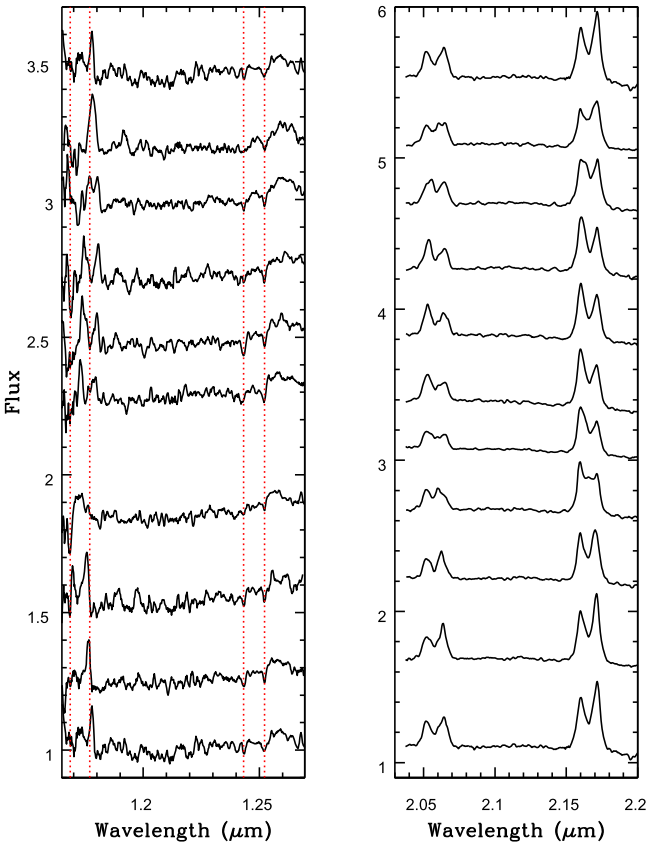

Figure 4. Gemini GNIRS *J*-band data (left hand panel), and the Keck NIRSPEC *K*-band spectra (right hand panel, from Harrison 2016a) for WZ Sge. The changing morphology of the unidentified emission line at 1.1758 μm mimics that of the He I and H I lines in the *K*-band, except that the absorption from the K I doublet (dotted red vertical lines) in the donor star strongly perverts its profile. The separation between the two peaks of this line, $\Delta v = 1400$ km s^{-1}, is identical to that found for H I Brγ.
(A color version of this figure is available in the online journal.)

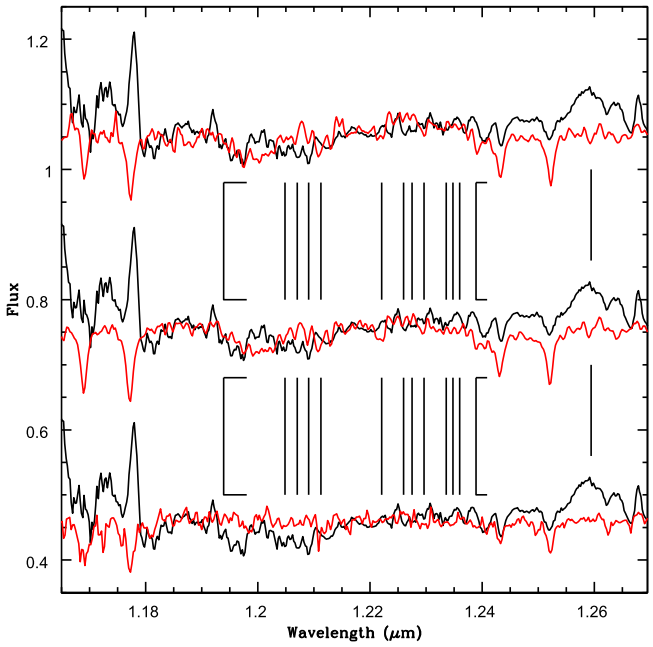

Figure 5. $\phi = 0$ spectrum of WZ Sge (black) compared to those of an L2 (Kelu 1, top), an L5 (2MASS1507−1627, middle), and an L8 (DENISJ0255–4700, bottom) from the IRTF Spectral Library (Cushing et al. 2005). We mark the positions of the most prominent FeH absorption features with vertical lines. Two bandheads from the $F^4\Delta$–$X^4\Delta$ system (see Cushing et al. 2003), the 0−1 at 1.1939 μm, and the 1−2 at 1.2389 μm, have their full extent detailed.
(A color version of this figure is available in the online journal.)

Given that much of the line emission region is eclipsed near $\phi = 0$, we concentrate on the spectrum obtained at this phase. In Figure 5, we compare the (boxcar smoothed) spectrum of WZ Sge with those of an L2 (Kelu 1), L5 (2MASS1507 −1627), and L8 (DENISJ0255-4700) from the IRTF Spectral Library (Cushing et al. 2005). The $\phi = 0$ spectrum of WZ Sge presented in Figure 5 has a S/N $\sim$ 60 at 1.2 μm. With the lack of strong telluric features in this bandpass, most of the structure seen in this, and the other spectra for WZ Sge is real. We delineate the location of the FeH features in Figure 5 for this bandpass as tabulated in Cushing et al. (2003). It is clear that much of the FeH absorption in WZ Sge is of a similar strength to that seen in the early to mid-L dwarfs. What is peculiar about the spectrum of the donor star in WZ Sge is the weakness of the red K I doublet. The corruption of the unidentified emission feature by the *blue* K I doublets suggest they are of a similar depth as the individual emission peaks, and are consistent with those of an early/mid L dwarf.

To further explore why the spectrum of WZ Sge differs from that of the L dwarf templates, it is useful to compare its spectrum to the *J*-band data of other CVs with strong accretion disk emission. In Figure 6 we plot the spectra of WZ Sge at the cardinal phases along with spectra of LS Peg and V603 Aql (from Harrison 2016b, and Harrison et al. 2007, respectively). Both of these CVs have much longer orbital periods than WZ Sge ($P_{\rm LSPeg} = 4.2$ hr, $P_{\rm V603Aql} = 3.3$ hr), but both have near-infrared spectra dominated by hydrogen and helium emission like WZ Sge. As can be seen in Figure 5, the FeH (0−1) bandhead at 1.194 μm in WZ Sge has a small emission bump at 1.2 μm that ruins the match of the template spectra to that of WZ Sge. The source of this feature is an He I emission line at 1.1989 μm that is clearly visible in the spectra of LS Peg and V603 Aql. Note that for V603 Aql, we have offset the observed spectrum by $\pm$28 Å, and then summed the two shifted spectra to construct a spectrum with double-peaked emission line profiles similar to those seen for He I in WZ Sge. Given that the red components of the double peaked emission lines in WZ Sge are much stronger than the blue components at $\phi = 0$ (see Figure 4), the entire bump at 1.2 μm inside the FeH

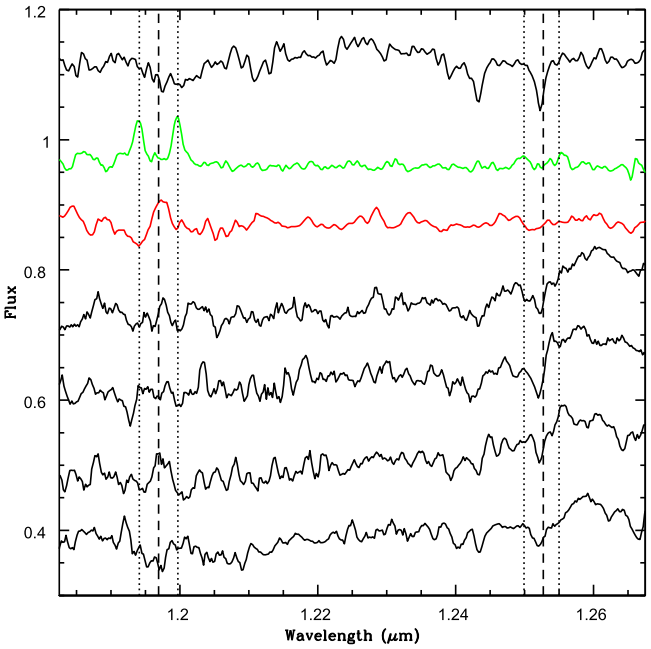

Figure 6. GNIRS spectra of WZ Sge (black, from the bottom) at $\phi = 0.0$, 0.25, 0.5 and 0.75. We plot the spectra of LS Peg in red, V603 Aql in green, and Kelu 1 (top, black). To mimic the line profiles of H I seen in WZ Sge, we have offset the spectrum of V603 Aql by +28 and −28 Å, and summed those two spectra together. The vertical dashed lines are the locations of the centers of the two H I lines. The dotted lines locate the expected positions of the blue and red emission components of H I lines in WZ Sge.
(A color version of this figure is available in the online journal.)

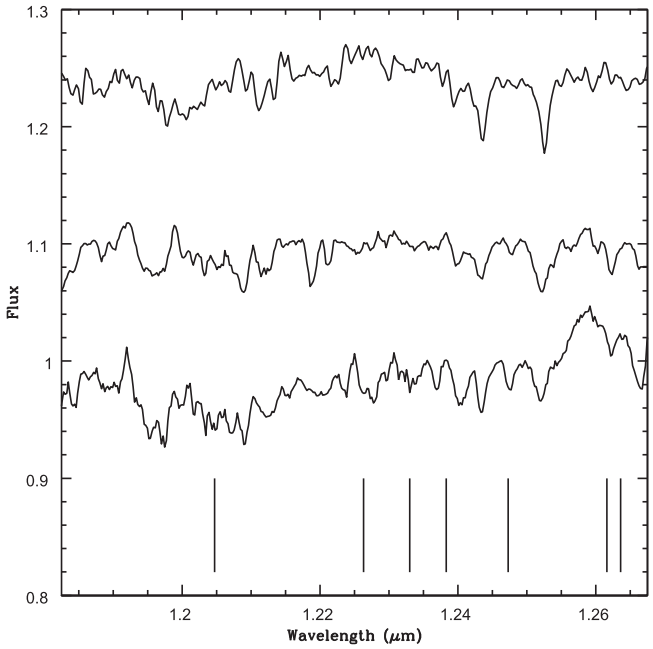

Figure 7. At the bottom is the $\phi = 0$ spectrum of WZ Sge. The locations of lines from H_2 are identified using vertical solid lines (from Aleman & Gruenwald 2011). The second spectrum from the bottom is the result of fitting a sixth order polynomial to the continuum of the $\phi = 0$ spectrum WZ Sge, and dividing it out. The top spectrum is that of Kelu 1.

feature is easily explained as arising from this He I line. The result is a relatively normal L dwarf FeH feature for the donor in WZ Sge. Both V603 Aql and LS Peg appear to have additional weak emission features in the 1.225–1.245 μm bandpass that also appear to be present in WZ Sge.

The more peculiar aspect of the WZ Sge spectrum occurs at the red end of the GNIRS data set. The red K I doublet is much weaker in the donor of WZ Sge when compared to any of the early/mid-L dwarf templates. In fact, the strength of the K I lines are more similar to those seen in L8 dwarfs. Given the rise of the continuum to the red that starts near 1.24 μm, some other emission line, or combination of lines, are contaminating the K I doublet. The spectrum of V603 Aql shows an emission feature centered at 1.2528 μm that is due to H I. In fact, this line is almost exactly at the same wavelength as the redder of the two K I lines (λ1.2522 μm). The effect of this emission line can be seen in the changing depth of the K I line as the H I emission moves as the orbital phase changes. This line, however, is probably much too weak to explain the shallowness of *both* of the components of the K I doublet (its strength is best visualized in the $\phi = 0.75$ spectrum in Figure 6).

The source of the dilution of the redder K I doublet is clearly the broad emission feature that is centered near 1.26 μm. This feature is much broader than can be explained by a single atomic emission line, and suggests molecular emission. There are some extremely weak CO bandheads at the red end of the *J*-band that arise from the third overtone rovibrational transitions (Li et al. 2015). Any such lines, however, should be very weak: $\sim 10^{-4}$ that of the first overtone features seen in the *K*-band (Tan et al. 2017). We are not aware of the detection of either absorption or emission lines from these third overtone transitions of CO in any astronomical object. Molecular hydrogen, seen in emission in the *K*-band spectra of WZ Sge presented by Howell et al. (2004), has lines at 1.2616 and 1.2636 μm, as well to the blue of these two lines (see Figure 7). Perhaps the sum of velocity broadened, double-peaked emission line profiles for all of the H_2 lines in this region might reproduce the observed broad feature. Emission lines from H_2 in the *J*-band are not often seen, with detections primarily confined to spectra of active galactic nuclei. However, the "4−2 S(3)" line of H_2 at 1.2616 μm is relatively strong in the spectra of some reflection nebulae (e.g., NGC 1333, see Martini et al. 1999).

Since the identification of this feature is mysterious, we have simply decided to remove it by fitting a sixth order polynomial to the continuum, and dividing it into the $\phi = 0$ spectrum. The result of this operation is shown in Figure 7, where we again plot the spectrum of Kelu 1. The depths of the two K I lines are now closer to those of an L2 dwarf. Note that the redder of

these two lines is still contaminated by weak H I emission. The K I lines in the subtracted spectrum appear to be broader than those of Kelu 1. Kelu 1 has a rotation rate of $v \sin i = 69\,\mathrm{km\,s^{-1}}$ (Blake et al. 2010). With the constraint on the radial velocity derived above, to contain a white dwarf in the mass range $0.6\,M_\odot \leqslant M_1 \leqslant 1.3\,M_\odot$ in the WZ Sge system, the rotation rate of the donor has to be in the range $120\,\mathrm{km\,s^{-1}}$ to $90\,\mathrm{km\,s^{-1}}$.

4. Discussion and Conclusions

The radial velocity curve, and tentative identification of the donor in WZ Sge as an L dwarf (Harrison 2016a), suggested that observations in the *J*-band might lead to both a better radial velocity curve and a more precise spectral type. While we have accomplished the former, the spectral type of the donor in WZ Sge has not been clarified. The presence of weak He I emission at critical wavelengths in the GNIRS spectra, and a broad feature at the red end of the data set, have made a refined classification of the donor impossible. Given the lack of useful spectral typing features anywhere else in the near-infrared, it appears that additional attempts to refine its classification will likely prove unfruitful.

The radial velocity semi-amplitude derived above leads to a mass function of $f(M_1) = 0.85 \pm 0.05\,M_\odot$. This suggests that the white dwarf in WZ Sge is more massive than found in model predictions (de Kool 1992; Politano 1996), but is completely consistent with previous findings that the white dwarfs in CVs are more massive than isolated, field white dwarfs (see Savoury et al. 2011, and references therein). Steeghs et al. (2001) found a radial velocity semi-amplitude for the primary in WZ Sge of $K_1 = 37 \pm 5\,\mathrm{km\,s^{-1}}$ by finding the center of symmetry in an Hα tomogram. Due to systematic effects in the line emission, they believed this was an upper limit. Assuming this value, the mass ratio for WZ Sge is $q = M_2/M_1 \leqslant 0.070$. Steeghs et al. (2007) directly detected UV absorption lines that led to a velocity of $K_1 = 47 \pm 3\,\mathrm{km\,s^{-1}}$. This gives a mass ratio of $q = 0.09$. They also derived a white dwarf mass of $0.84 \pm 0.04\,M_\odot$ by inferring that the difference between the observed mean velocity of the white dwarf and the systemic velocity was due to the gravitational redshift of the primary. Skidmore et al. (2002) found a value of $M_1 = 0.82 \pm 0.10\,M_\odot$ by assuming the outer edge of the accretion disk in WZ Sge is at the 3:1 tidal resonance, and orbits with a velocity of $723\,\mathrm{km\,s^{-1}}$. These two values for the primary mass are in agreement with our mass function determination.

It is unlikely that WZ Sge was born with an L-dwarf donor star. Thus, the present object may look like an L dwarf, but has had a dramatically different history. The spectral type of an L dwarf is highly dependent on its age (see Baraffe et al. 2015). We presume that the donor in WZ Sge more closely resembles older brown dwarfs, and has no internal sources of energy. For the spectral type limits we have derived, the typical mass of an older L dwarf is $70\,M_{\mathrm{Jup}} = 0.067\,M_\odot$ (Dupuy & Liu 2017). If we assume that this is true for the donor in WZ Sge, the mass ratio is $q = 0.067/0.84 = 0.080$. Using $K_1 = 47\,\mathrm{km\,s^{-1}}$, $K_2 = 525\,\mathrm{km\,s^{-1}}$, and $M_2 = 0.067\,M_\odot$, gives $M_1 = 0.75\,M_\odot$. It appears that both the gravitational redshift mass and the mass inferred from the UV absorption line radial velocity curve are consistent with each other, and the masses of the two components that comprise WZ Sge are not especially unusual.

Attempts have been made to use the period of the superhumps, seen in the outburst light curves of short period ("SU UMa") CVs, to constrain their mass ratios. Patterson (1998) found a limit of $q < 0.043(M_1/0.7\,M_\odot)^{-1/3}$ for WZ Sge, while Kato (2015) found $q = 0.078$. The Patterson estimate leads to $K_1 \leqslant 24\,\mathrm{km\,s^{-1}}$, and that of Kato to $K_1 = 41\,\mathrm{km\,s^{-1}}$. Both are consistent with the derivation by Steeghs et al. (2001), but only that from Kato is marginally consistent with the result from Steeghs et al. (2007).

The lack of tighter constraints on the spectral type of the donor in WZ Sge is disappointing. If we assume that the donor in WZ Sge is a completely normal L dwarf, we can estimate its contribution to the luminosity of WZ Sge. Kelu 1 is a binary brown dwarf consisting of an L2 and and an L4 (Liu & Leggett 2005) at a distance of 18.7 pc. In the *J*-band they differ by $\Delta J = 0.67$ mag. Kelu 1a has $J = 15.5$, while during eclipse, WZ Sge has $J = 14.9$ (Harrison et al. 2013). This indicates that Kelu 1a at the distance of WZ Sge would supply 57% of the total *J*-band flux. Given that the spectrum of WZ Sge is relatively blue, and the spectra of L dwarfs are red, we estimate that at 1.2 μm, Kelu 1a would supply ≈67% of the flux in the bandpass of the GNIRS data. Given that an L5 dwarf is 0.85 mag fainter in the *J*-band than an L2, it would seem unlikely that such an object could supply sufficient luminosity to explain our observations, and thus an early L dwarf donor appears more credible. The difficulty with such inferences is that the donor in WZ Sge has a history that is unlike any field L dwarf, and it is probably dangerous to assume that the secondary in WZ Sge closely resembles such objects.

In conclusion, after a multi-decade effort to characterize its donor, the underlying nature of the stellar components in WZ Sge appears to be solved. If Knigge et al. (2011) are correct, WZ Sge does not appear to be a period bouncer. For objects with the orbital period of WZ Sge ($P_{\mathrm{orb}} = 1.36$ hr), Knigge et al. would predict (see their Table 6) that the donor star would have a mass of $0.06\,M_\odot$, and a temperature of 2100 K. This is very similar to what we have inferred for WZ Sge. They predict that period bouncers have lower masses and temperatures than that found for the donor in WZ Sge. This conclusion is strengthen by the comparison of our measured value of the mass ratio, $q = 0.09$, to the values Patterson (2011) expects for true period bounce systems. In his Figure 6, period bounce systems are expected to have $q \simeq 0.05$. A value of $q = 0.09$ would indicate a system still evolving toward the period minimum.

The presence of low level emission from He I, and an unidentified source in the red end of the GNIRS data set, has compromised our ability to narrow down the spectral classification of the donor. While it appears unlikely that future observations will provide additional insight into the donor's temperature, the origin of the broad emission feature at 1.26 μm warrants further investigation. The most plausible explanation is H_2 emission. Molecular hydrogen emission was observed in the *K*-band by Howell et al. (2004), but was not seen in spectra of WZ Sge obtained one year later (Harrison 2016a). Perhaps this emission is transient, occasionally allowing for a better view of the redder K I doublet. Fortunately, this unidentified emission feature does not appear to preclude the future use of the red K I doublet to measure $v_{\rm rot}$ sin*i* of the companion in WZ Sge, enabling a direct measurement of the mass of the primary. This would allow for an additional check on the white dwarf mass in WZ Sge.

T.E.H. was partially supported by a grant from the NSF (AST-1209451). The Gemini GNIRS data were acquired under the program GN-2016B-Q-69.

References

Aleman, I., & Gruenwald, R. 2011, A&A, 528, 74
Baraffe, I., Homeier, D., Allard, F., & Chabrier, G. 2015, A&A, 577, A42
Blake, C. H., Charbonneau, D., & White, R. J. 2010, ApJ, 723, 684
Cushing, M. C., Rayner, J. T, Davis, S. P., & Vacca, W. D. 2003, ApJ, 582, 1066
Cushing, M. C., Rayner, J. T, & Vacca, W. D. 2005, ApJ, 623, 1115
Davey, S., & Connon Smith, R. 1992, MNRAS, 257, 476
de Kool, M. 1992, A&A, 261, 188
Dupuy, T. J., & Liu, M. C. 2017, arXiv:1703.05775
Harrison, T. E. 2016a, ApJ, 816, 4
Harrison, T. E. 2016b, ApJ, 833, 14
Harrison, T. E., Campbell, R. K., Howell, S. B., Cordova, F. A., & Schwope, A. D. 2007, ApJ, 656, 444
Harrison, T. E., Hamilton, R. T., Tappert, C., Hoffman, D. I., & Campbell, R. K. 2013, AJ, 145, 19
Harrison, T. E., Johnson, J. J., McArthur, B. E., et al. 2004, AJ, 127, 460
Howell, S. B., Adamson, A., & Steeghs, D. 2003, A&A, 399, 219
Howell, S. B., Harrison, T. E., & Szkody, P. 2004, ApJL, 602, L49
Kato, T. 2015, PASJ, 67, 108
King, A. R., & Kolb, U. 1995, ApJ, 439, 330
Knigge, C., Baraffe, I., & Patterson, J. 2011, ApJS, 194, 28
Kolb, U., & Baraffe, I. 1999, MNRAS, 309, 1034
Li, G., Gordon, I. E., Rothman, L. S., et al. 2015, ApJS, 216, 15
Liu, M. C., & Leggett, S. K. 2005, ApJ, 634, 616
Martini, P., Sellgren, K., & DePoy, D. L. 1999, ApJ, 526, 772
McGovern, M. R., Kirkpatrick, J. D., McLean, I. S., et al. 2004, ApJ, 600, 1020
McLean, I. S., McGovern, M. R., Burgasser, A. J., et al. 2003, ApJ, 596, 561
McLean, I. S., Prato, L., McGovern, M. R., et al. 2007, ApJ, 658, 1217
Patterson, J. 1998, PASP, 110, 1132
Patterson, J. 2011, MNRAS, 411, 2965
Patterson, J., Gianluca, M., Richmond, M. W., et al. 2002, PASP, 114, 721
Patterson, J., Richman, H., Kemp, J., & Mukai, K. 1998, PASP, 110, 403
Politano, M. 1996, ApJ, 465, 338
Savoury, C. D. J., Littlefair, S. P., Dhillon, V. S., et al. 2011, MNRAS, 415, 2025
Skidmore, W., Wynn, G. A., Leach, R., & Jameson, R. F. 2002, MNRAS, 336, 1223
Steeghs, D., Howell, S. B., Knigge, C., et al. 2007, ApJ, 667, 442
Steeghs, D., Marsh, T., Knigge, C., et al. 2001, ApJL, 562, L145
Tan, Y., Wang, J., Zhao, X.-Q., Liu, A.-W., & Hu, S.-M. 2017, JQSRT, 187, 274
Thorstensen, J. R. 2003, AJ, 126, 3017